Urgent neonatal balloon atrial septostomy in simple transposition of the great arteries: predictive value of fetal cardiac parameters

O. Patey[1,2,3], J.S. Carvalho[1,2,3]#, and B. Thilaganathan[1,2]#

Joint senior authorship#

[1]Molecular & Clinical Sciences Research Institute, St George's University of London, UK;

[2]Fetal Medicine Unit, St George's University Hospitals NHS Foundation Trust, London, UK;

[3]Brompton Centre for Fetal Cardiology, Royal Brompton and Harefield Hospitals NHS Foundation Trust, London, UK

Author for correspondence

Dr Olga Patey

Fetal Medicine Unit

4th Floor, Lanesborough Wing

St George's University Hospitals NHS Foundation Trust

London SW17 0QT

Email: pateyolga@gmail.com

Short title: Fetal cardiac predictors for neonatal BAS in simple TGA

Keywords: Balloon atrial septostomy; fetal heart; echocardiography; left ventricular rotation, twist and torsion; prediction; speckle tracking; tissue Doppler imaging; transposition of the great arteries.

This article has been accepted for publication and undergone full peer review but has not been through the copyediting, typesetting, pagination and proofreading process which may lead to differences between this version and the Version of Record. Please cite this article as doi: 10.1002/uog.22164

Contribution

What are the novel findings of this work?

The proposed novel fetal cardiac indices showed high sensitivity and specificity for prediction an urgent balloon atrial septostomy (BAS) in TGA neonates suggestive of the impact of hypoxemia and unique haemodynamic loading conditions on cardiac remodelling and functional adaptation in simple TGA term fetuses.

What are the clinical implications of this work?

If our findings of predictive values of fetal cardiac parameters for emergency BAS in TGA neonates are validated in larger prospective studies, a detailed cardiac assessment of TGA fetuses near term could facilitate improvement of perinatal management and refining the timing of postnatal intervention strategies to prevent adverse pregnancy outcome

ABSTRACT

Aims: 1) To investigate the impact of abnormal perinatal loading conditions on cardiac geometry and function in transposition of the great arteries with intact interventricular septum (simple TGA) term fetuses and neonates, 2) to explore predictive values of fetal cardiac parameters for an urgent balloon atrial septostomy (BAS) in TGA neonates.

Methods: Prospective longitudinal follow up study of 67 women delivering at term including 54 uncomplicated pregnancies with normal outcome and 13 pregnancies affected by fetal simple TGA. Conventional, spectral tissue Doppler imaging and speckle tracking echocardiographic parameters were obtained within one week before delivery and a first few days after birth. Neonatal assessments were done after urgent BAS and before corrective arterial switch surgery.

Results: Compared to normal pregnancy, TGA term fetuses exhibited more globular hypertrophied ventricles, increased biventricular systolic function and diastolic dysfunction (right ventricular [RV] sphericity index [SI]: 0.54 vs. 0.58; left ventricular [LV] SI: 0.49 vs. 0.55, combined cardiac output [CCO]: 406ml/min/kg vs. 483ml/min/kg, LV torsion 3.0deg/cm vs. 4.3deg/cm, RV isovolumetric relaxation time [IVRT']: 102ms vs. 127ms, $p<0.010$ for all). TGA neonates demonstrated biventricular hypertrophy, more spherical right ventricle and altered systolic and diastolic functional parameters (RV SI: 0.43 vs. 0.61, RV myocardial performance index [MPI']: 0.34 vs. 0.47, CCO: 486ml/min/kg vs. 697ml/min/kg, LV IVRT': 79ms vs. 100ms, RV IVRT': 71ms vs. 106ms, $p<0.001$ for all). Paired comparison of fetal and neonatal cardiac indices in TGA group showed persistence of the fetal phenotype, increased biventricular systolic myocardial contractility and CCO, and diastolic dysfunction (RV myocardial longitudinal systolic velocities [S']: 6.8cm/s vs. 9.0cm/s, LV S': 5.0cm/s vs. 6.0cm/s, LV torsion: 4.3deg/cm vs. 1.1deg/cm, $p<0.001$ for all). Several fetal cardiac parameters in TGA term

fetuses revealed high predictive values for urgent BAS procedure after birth: LV rotation-to-shortening ratio [RSR] - our proposed novel fetal cardiac index as a potential marker of subendocardial dysfunction (the cut-off value ≥0.23, area under curve [AUC]=0.94, sensitivity=100%, specificity=83%), and RV/LV end-diastolic area ratio ≥1.33, pulmonary valve to aortic valve dimension ratio ≤0.89, RV/LV CO ratio ≥1.38, and foramen ovale (FO) dimension to total interatrial septal length ratio ≤0.27 (AUC=0.93-0.98, sensitivity=86%, specificity=83%-100% for all).

Conclusions: Simple TGA fetuses exhibited cardiac remodelling at term with more profound alterations in these cardiac parameters after birth suggestive of adaptation to abnormal loading conditions and possible adaptive responses to hypoxemia. Perinatal adaptation in TGA might reflect persistence of the abnormal parallel arrangement of cardiovascular circulation and presence of widely patent fetal shunts imposing volume load on the neonatal heart. The fetal cardiac parameters that showed high predictive values for urgent BAS in TGA neonates might reflect the impact of late-gestation pathophysiology and progressive hypoxemia on fetal cardiac geometry and function. If these findings are validated in larger prospective studies, the detailed cardiac assessment of TGA fetuses near term could facilitate improvement of perinatal management and refining the timing of postnatal intervention strategies to prevent adverse pregnancy outcome.

INTRODUCTION

Complete transposition of the great arteries (TGA) is a group of congenital cardiac defects characterized by atrioventricular concordance and ventriculoarterial discordance, and is one of the most common cyanotic heart defects accounting for 10% of all neonatal cyanotic cardiac malformations [1-3]. TGA with intact interventricular septum (simple TGA) is a very specific abnormality in which the changes in fetal cardiovascular circulation around the time of birth maybe associated with the restriction of the foramen ovale (FO) and/or ductus arteriosus [4-12] and blood flow redistribution [7, 13-16], and subsequent development of severe hypoxemia postnatally leading to rapid haemodynamic compromise and perinatal complications [17, 18]. The premature shunt restriction in simple TGA fetuses requires an urgent balloon atrial septostomy (BAS) performed in the first 24 hours after birth. Even with prenatal diagnosis of simple TGA, prediction of postnatal instability in neonates may be difficult [19]. We hypothesized that cardiovascular adaptation to blood flow redistribution in simple TGA at term could lead to altered loading conditions faced by ventricles, thus affecting cardiac geometry and myocardial contractility. In spite of modern cardiac technologies such as tissue Doppler and speckle tracking echocardiography (STE) which demonstrated better sensitivity for detection of subtle subclinical changes in myocardial contractility in fetuses [20, 21], there is paucity of data on the cardiac functional assessment of simple TGA term fetuses due to the lack of studies performed at the critical period near term, retrospective study design , and application only conventional echocardiographic techniques with controversial findings [8, 10, 13-16]. Some data are available on evaluation of neonatal cardiac geometry and function but results are conflicting with only three of these studies using modern ultrasound modalities [16, 22-25]. Prediction of urgent BAS intervention after birth has not been fully elucidated and relied on retrospective fetal cardiac measurements that produced conflicting reports [4-10, 12]. The comprehensive evaluation of

perinatal cardiac changes in TGA term fetuses with both conventional and modern ultrasound modalities may help better understanding of this congenital heart malformation pathophysiology, whereas prenatal prediction of an urgent BAS in neonates may help in optimizing perinatal management, pregnancy outcome and reducing the risks of postnatal cardiovascular complications.

PATIENTS AND METHODS

Study Population

This was a prospective longitudinal study of singleton pregnancies at term including two patient groups: uncomplicated pregnancies with normal outcome and those affected by TGA. For the control group, pregnant women attending for routine antenatal care at St. George's Hospital were enrolled if the pregnancies were assessed as normal and fetuses had structurally normal hearts. Pregnant women with a confirmed diagnosis of fetal simple TGA were recruited in the Fetal Cardiology clinic at the Fetal Medicine Unit at St. George's Hospital between July 2014 and September 2016. They were asked to participate in this study if the fetuses did not have any extracardiac structural and chromosomal abnormalities or impaired fetal growth, and any maternal pre-pregnancy or pregnancy-related co-morbidity. The neonatal assessment was conducted in the Paediatric Cardiology department at the Royal Brompton Hospital. All participants gave written informed consents for fetal and neonatal cardiac assessment. The Ethics Committee of NRES Committee London-Surrey Borders approved the study protocol (Reference -12/LO/0945).

Echocardiography

Fetal B-mode, M-mode, spectral pulsed-wave (PW) Doppler, spectral tissue Doppler imaging (PW-TDI) and speckle tracking echocardiography (STE) were performed a few days before birth. The neonatal cardiac assessment was conducted within hours after birth. There were no patients excluded from the study because data could not be acquired. Prostaglandin therapy was begun immediately after birth in all TGA neonates to keep the patency of the ductus arteriosus. TGA neonates required urgent BAS were scanned within 24 hours after the intervention. TGA newborns with non-restrictive FO that did not require BAS were receiving

prostaglandin therapy at the time of the neonatal scan. Thus, both interatrial communication and PDA were widely patent in all TGA neonates at the time of postnatal scans. One investigator (OP) performed all fetal and neonatal ultrasound examinations using the same ultrasound system Vivid E9 (General Electric, Zipf, Austria) at both hospital sites. Fetal M-mode, B-mode, and PW Doppler measurements were made with the convex array obstetric transducer 4C, while the paediatric/neonatal cardiac sector probe 12S was used for neonatal heart examination. PW-TDI curves and 2D images for STE analysis were obtained and recorded in the same manner and with the same linear ultrasound transducer M5S in both fetal and neonatal groups. *M-mode* ultrasound was used for assessment of cardiac geometry and function and ventricular longitudinal axis annular plan systolic motion. *B-mode* imaging was performed for obtaining measurements of the cardiac valve and end-diastolic ventricular dimensions and areas, and calculation of ventricular sphericity index (sphericity index= ventricular end-diastolic dimension/end-diastolic length). Relative wall thickness of the ventricles and interventricular septum was estimated as twice free wall thickness or septum thickness divided by ventricular end-diastolic diameter [26]. The dimensions of FO to the total inter-atrial septum length (TSL) were measured for calculation of FO/TSL ratio as previously described [8] but with our modification of FO dimension measurements as a size of an effective shunt across the interatrial septum visualised on 2D and confirmed by colour Doppler technique. Additionally, appearance of and interatrial septum was examined and defined according to the previously published criteria: redundant, if aneurysmal septum primum bulged 50% of the way to the left atrial free wall; flat, if the angle between the septum primum and the rest of the atrial septum was <30 ; fixed, if the septum primum did not show the typical swinging motion during the cardiac cycle; hypermobile, if the septum primum flap oscillated between both atria [6, 8, 9, 12, 27]. The ductus arteriosus shunting pattern was described as antegrade

(forward flow) or retrograde (reversed flow) [6, 9]. *Pulsed wave (PW) Doppler* technique was used to obtain Doppler signals from the inflow and outflow tracts for evaluation of diastolic and systolic function respectively and calculation of stroke volume (SV) and cardiac output (CO). Angle correction was used for the alignment of an ultrasound beam with a blood flow because of a variation in fetal positions. *PW-tissue Doppler (PW-TDI)* technique was applied to derive cardiac indices of myocardial motion in systole and diastole, and for measurement of myocardial time-interval parameters allowing estimation of left ventricular (LV) and right ventricular (RV) myocardial performance index (MPI'). *Speckle tracking echocardiography (STE)* was used to derive all aspects of global and regional myocardial deformation (longitudinal, circumferential, radial and rotational) with a frame rate greater than 100 frames per second (fps). Digital clips were obtained, serially numbered and anonymized patient data were then transferred to the dedicated software EchoPAC (version 112, GE Medical System) for further analysis. The novel fetal cardiac index - *LV rotation-to-shortening ratio (RSR)* - as a potential index of LV subendocardial dysfunction [28, 29] was modified for the fetal heart assessment with respect to the known variation of twist patterns in term fetuses [30]. It was calculated by dividing LV apical rotation by LV basal circumferential strain. All echocardiographic measurements were performed according to the standardized protocol of the study and with regards to previously described fetal echo techniques [30-33] (Supplemental data). The time-interval values were adjusted by cardiac cycle length normalizing for the difference in heart rate. Other fetal and neonatal indices were normalized by dividing corresponding measurements by the ventricular length or end-diastolic dimension according to the study methodology and previous publications [30-34]. The detailed analysis of the intra- and inter-observer reproducibility on the ultrasound machine utilized for this study was reported previously [32, 33, 35] and summarised in Supplemental data.

Statistical Analysis

For strain rate as a primary outcome, a sample of 26 (13 normal and 13 with fetal TGA pregnancies) would detect a rate of change (length/s) difference of 0.24 (equivalent to 10% of the mean, 2.44), with power of 80%, significance level of 5%, and assuming a standard deviation of 0.24. To allow for possible confounding factors including dropouts, this number was doubled for normal pregnancies. Statistical analysis was performed using SPSS version 22.0 (SPSS Inc., Chicago, IL, USA). Both Shapiro-Wilk test and Kolmogorov-Smirnov test were performed to assess the data for normality. For normally distributed data, paired T-test and independent sample T-tests to compare fetal and neonatal cardiac variables were performed as appropriate. For skewed data, Wilcoxon sign rank for paired data and Mann-Whitney tests for unpaired comparisons were used. The categorical data were compared using Pearson's Chi-square test. The differences between groups were deemed as significant only if the 2-tailed p-values were less than 0.01 (Bonferroni correction for type 1 error or false positive results of multiple measurements). Additionally, the Receiver Operating Characteristic (ROC) curve analysis with calculations of sensitivity and specificity of fetal cardiac parameters and their cut-off values for prediction of BAS outcome in TGA neonates was conducted.

RESULTS

Maternal demographic characteristics and pregnancy details are summarized in Table 1. A total of 67 pregnant women delivering at term consented to the study (54 normal pregnancies and 13 with a diagnosis of fetal simple TGA). Postnatal scan assessment confirmed the prenatal diagnosis of TGA as well as a very small (1.5mm) perimembranous ventricular septal defect in two fetuses with TGA that were diagnosed prenatally. A restrictive FO was diagnosed in 7 (54%) term TGA fetuses, but no cases of restrictive ductus arteriosus. After birth, a FO restriction was found in 7 (54%) of neonates that required emergency BAS. The restrictive flow across the interatrial septum diagnosed prenatally was confirmed in 6 fetuses; there were one false negative and one false positive outcomes. Two neonates with restrictive FO had also a restriction of ductus arteriosus in the first hours after birth, that was not seen at the time of scan at 37-38 weeks of gestation. There were two cases of neonatal pulmonary hypertension that required emergency BAS. One of the cases had only restrictive FO, where the other case had both FO and ductus arteriosus restriction. There were no cases with prenatal administration of corticosteroids in our study. Oxygen was administrated to all TGA neonates after birth, whereas none required inotropic support. The need for emergency BAS was based on a combination of clinical presentation of significant systemic hypoxemia (preductal oxygen saturations <60%) in neonates on prostaglandin and restrictive flow across the interatrial septum on postnatal echocardiography. The neonates were intubated and sedated during BAS procedure. The maternal/fetal/neonatal characteristics, duration of ventilation, prostaglandin E and oxygen need, and timing of echocardiographic evaluation did not differ between TGA cases that required BAS procedure [BAS subgroup] and those that did not have this intervention [non-BAS subgroup] (Supplemental Table S1). Subsequently, all TGA neonates underwent arterial switch operation with the live outcomes.

Cardiac Geometry

TGA fetuses demonstrated significantly decreased both LV and RV end-diastolic lengths (EDL) with resulting significantly increased LV and RV sphericity indices compared to normal term fetuses. There was an increase in relative thickness of IVS, LV and RV walls and aortic valve (AV) dimensions, whereas pulmonary valve (PV) to AV dimension ratio was decreased (Figure S1, Tables 2 and S2). TGA newborns showed decreased left atrioventricular valve (AVV) measurements, LV end-diastolic dimensions (EDD), LV and RV EDL and PV size, while the following indices were significantly increased: right AVV dimension, RV EDD, RV sphericity index, the relative thickness of LV and RV walls and IVS, and AV dimension (Figure S1, Tables 2 and S2). Perinatal changes in cardiac geometry in TGA group did not show any significant alterations (Figure S1, Tables 2 and S2).

Global Myocardial Deformation and Performance

TGA fetuses showed increased RV longitudinal strain, LV basal circumferential and basal radial strain/systolic strain rate values with an elevated LV torsion (Figure 1, Tables 3 and S2). In comparison to the normal newborns, TGA neonates demonstrated significantly increased both LV and RV longitudinal strain rates, LV basal and apical circumferential strain/systolic strain rates, and LV basal radial strain/systolic strain rates (Figure 1 and Table S2). There was also significantly increased RV and LV myocardial performance index (MPI'), and LV and IVS annular plane longitudinal systolic motion (Table 3 and S2). Perinatal changes in TGA group showed a significant increase in LV basal circumferential strain and basal radial strain and reduced LV torsion (Figure 1, Tables 3 and S2).

Systolic Function

TGA fetuses revealed significantly increased both LV and RV ejection time periods, RV systolic myocardial velocities S' with increased both RV CO and combined cardiac outputs (CCO) (Figure S1, Tables 3 and S2). TGA neonates differed from the normal group by significantly increased heart rate, LV CO, RV CO, CCO, LV ejection time (ET') periods, both LV and RV isovolumetric contraction times (IVCT') and LV, RV, and IVS myocardial systolic annular velocities S' (Figure S1, Tables 3 and S2). Perinatal changes in TGA group revealed a significant increase in CCO at the expense of an increase in both LV and RV output without change in fetal heart rate, and a significant perinatal increase in RV ET' and LV, RV and IVS myocardial longitudinal systolic velocities S' (Figure S1, Tables 3 and S2).

Diastolic Function

In comparison to normal fetuses, TGA fetal group demonstrated a significantly prolonged RV isovolumetric relaxation time (IVRT') and decreased both LV and RV relaxation time (RT') intervals (Figure S1, Tables 3 and S2). Postnatally, in comparison to normal newborns, TGA neonates had significantly lower values of LV and RV E/A and E'/A' ratios (both ratios<1), and decreased both LV and RV RT', while both LV and RV IVRT' were increased (Figure S1, Tables 3 and S2). Perinatal changes showed persistence of biventricular diastolic dysfunction (Figure S1, Tables 3 and S2).

A summary of alterations in cardiac parameters in TGA term fetuses and neonates compared to normal groups and perinatal changes in TGA group is presented in Figure 2 and Table 4. Reproducibility study results are summarized in Table S3 as previously reported [32, 33, 35].

Fetal cardiac parameters predictive for urgent BAS in TGA neonates

Comparing TGA fetuses in the subgroups of BAS with non-BAS, several geometrical and functional cardiac parameters showed significant differences (Figures 3 and S2). Our proposed novel fetal index LV rotation-to-shortening ratio (RSR) with cut-off value $\geq$ 0.23 showed 100% sensitivity at a slight expense of specificity (83%) for prediction of an urgent BAS in neonates. The following fetal cardiac parameters also revealed high predictive values for BAS with sensitivity of 86% and specificity 86%-100% for all: RV/LV end-diastolic area ratio, PV/AV dimension ratio, RV/LV CO ratio, and FO/TSL ratio (Table 5 and Figure 4). There was a strong negative correlation of FO/TDL ratio with RV/LV CO and RV/LV end-diastolic area ratios (Figure S3). There were neither significant differences in prevalence of hypermobility, flat/fixed appearance, redundancy of the FO flap, nor alterations in a retrograde diastolic flow in ductus arteriosus in non-BAS vs. BAS subgroups (Table S1).

DISCUSSION

Simple TGA fetuses exhibited cardiac remodelling at term with more profound alterations in these cardiac parameters after birth suggestive of adaptation to abnormal loading conditions and responses to hypoxemia. The fetal cardiac parameters that showed high predictive values for urgent BAS reflect the impact of these pathophysiological changes on fetal cardiac geometry and function. If these findings are validated in larger prospective studies, detailed cardiac assessment of TGA fetuses near term could improve perinatal management and pregnancy outcomes.

Fetal Cardiac Geometry and Function

Current knowledge of cardiovascular circulation in fetuses with TGA is based on Professor Abraham Morris Rudolph's theoretical postulates, whereby preferential blood streaming through the ductus venosus across FO to the left heart delivers highly oxygenated blood to the pulmonary circulation and descending aorta [5]. He suggested that pulmonary artery oxygen saturation in fetal TGA is increased to more than 70% compared to 55% in normal fetuses (Figure 5). Both the fetal pulmonary circulation and ductus arteriosus become increasingly sensitive to the high oxygen content towards the end of gestation [18, 36], which may predispose to restriction of FO and ductus arteriosus at term [8, 4-8] and blood flow redistribution [7, 13-16]. Rudolph also proposed that blood flow to the right ventricle would have a low oxygen content, such that the saturation in the ascending aorta and cerebrovascular circulation would be as much as 20% lower than in the normal fetuses [5] (Figure 5). TGA term fetuses in our study revealed the more spherical hypertrophied RV and LV chambers and a significant increase in biventricular systolic contractility and LV torsion, facilitating an increase in RV CO and CCO and diastolic dysfunction. These findings support the theory that in TGA term fetuses, a higher

oxygen content of blood in the left heart and pulmonary artery lowers pulmonary vascular resistance with a subsequently increased pulmonary venous return thereby increasing LV preload [7, 14, 18, 37-39], whereas a smaller diameter of the ductus arteriosus occurring in the late pregnancy in proportion of TGA fetuses can lead to elevation of LV afterload [18, 38, 40] (Figure 6). The known afterload sensitivity of the fetal heart may limit the ability of the left ventricle to increase the cardiac output above the normal values found in our study [41, 42]. In comparison, an increased venous return from the lungs elevates of left atrial pressure resulting in a relative restriction of FO and reduction of the right-to-left shunting across the atrial septum, thereby increasing RV preload [8, 4-8], whilst RV afterload decreases because the right ventricle has to pump against a relatively low cerebrovascular resistance at term [43] (Figure 6). Our findings of significantly raised RV CO and CCO reflect an increased volume workload of the right ventricle delivering the blood flow towards the coronary and cerebrovascular circulation, and consistent with the recent MRI and echocardiographic Doppler studies [7, 15, 16]. Greater preload and/or afterload contribute to compensatory wall thickening and greater ventricular chamber sphericity observed in both left and right ventricles in TGA fetuses [20, 44-47]. The increased myocardial contractility is associated with a decreased capillary density coupled with impaired relaxation of the heart [48,49]. In concordance, our results revealed biventricular diastolic dysfunction in TGA term fetuses that was evident from reduced LV and RV relaxation time and prolonged RV IVRT'. Some previous publications reported the different ventricular morphology and myocardial time-interval values [16], and unchanged CCO with left CO preponderance in simple TGA fetuses[13, 14]. These discrepancies can be explained by the retrospective design of these studies, inclusion of fetuses less than 37 weeks and non-adjustment of myocardial time-intervals for the difference in fetal heart rate. Additionally, our TGA data showed an increase in an aortic to pulmonary valve ratio due to aortic valve

enlargement that can be indicative of a vessel size alterations as a consequence of embryologic pathogenesis [50], and also reflect an flow mediated vascular remodelling due to adverse haemodynamic loading conditions [14,16, 51].

Neonatal Cardiac Geometry and Function

TGA neonates (all under prostaglandin E perfusion) demonstrated profound changes in all cardiac indices. The observed alterations could reflect a persistent abnormal parallel circulation and ventricular adaptation to the altered haemodynamic load. Postnatal adjustments in vascular resistance resulting in an elevation in systemic vascular pressure would impose an additional afterload on the right ventricle contributing to the increased RV sphericity and chamber hypertrophy [52, 53]. In contrast, our findings of a smaller left ventricle compared to the normal neonatal heart may reflect a reduced LV afterload due to the fall in pulmonary vascular resistance. The presence of widely open FO and ductus arteriosus might be responsible for equalization of systemic and pulmonary pressures and volumes [39]. Therefore, both ventricles are subjects to an increased haemodynamic preload explaining the persistent globular morphology of the heart, increased heart rate, biventricular contractility and elevated both LV and RV CO in TGA neonates [16]. The unique ability of the postnatal right ventricle to significantly increase CO in presence of increased afterload was recently demonstrated in a lamb model of congenital heart defect [52, 54] and in agreement with our results in human TGA neonates. Diastolic function in TGA neonates was significantly reduced with more profound changes observed in RV myocardial performance. Patients with dominant postnatal right ventricle often develop progressive RV dysfunction over time that may be related to differences in morphology, genetic profile and haemodynamic exposure between left and right ventricles [55-59].

Perinatal Changes in TGA group

Perinatal cardiac changes from TGA fetus to TGA neonate differed from normal transitional cardiovascular adaptation we described previously [31] and revealed the unchanged fetal cardiac phenotype, significantly increased biventricular systolic contractility, reduced LV torsion reflecting deterioration of LV diastolic dysfunction, and elevated biventricular cardiac output. These alterations can be attributed to persistence of the abnormal parallel arrangement of cardiovascular circulation, and also presence of the widely patent ductus arteriosus and FO shunts imposing an additional hemodynamic volume load on the neonatal heart.

Predictive values of cardiac parameters in TGA term fetuses for neonatal emergency BAS

Prenatal prediction of urgent BAS procedure after birth relies on retrospective fetal echocardiographic studies performed before 37 weeks of gestation producing conflicting results [4-10, 12] (Table S4). Variability of FO and ductus arteriosus responses was thought to be related to the amount of umbilical venous blood passing through the ductus venosus [5, 18]. In our study, TGA fetuses in the BAS subgroup showed significantly increased RV/LV end-diastolic area ratio and decreased both PV/AV and FO/TSL dimension ratios reflecting reduced blood flow across a restrictive FO resulting in the increased blood flow to the right heart, RV enlargement and aortic dilatation [51]. Such pronounced blood flow redistribution toward the cerebrovascular circulation is also consistent with a compensatory response to hypoxemia [18, 60,61,62] (Figure 6). Moreover, fetal FO and ductus arteriosus restriction can lead to the same blood flowing between the lungs and the left ventricle with richly oxygenated blood

from placenta bypassing the left heart, thus creating an isolation of pulmonary circulation and pulmonary hypoxemia [7] (Figure 6). Fetuses in the BAS subgroup also had an increased RV/LV CO ratio at the expense of a significant fall in LV CO and reduced LV basal circumferential strain, thus revealing LV dysfunction from pulmonary hypoxemia and increased LV afterload due to ductus arteriosus constriction [29]. A significantly increased LV apical systolic rotation in these fetuses might reflect a compensatory mechanism for improving LV diastolic dysfunction as a result of the ventricular interaction where expansion of RV chamber causes an apparent decrease in LV compliance [30,63]. Elevated LV apical rotation can also be a result of an increased afterload faced by the left ventricle resulting in subendocardial microvascular insufficiency, increased oxygen demand and LV myocardial helical imbalance [29,30]. We proposed a novel modified index for fetal heart assessment, namely LV rotation-to-shortening ratio (RSR) as a ratio of apical systolic rotation to basal circumferential strain. RSR demonstrated the highest sensitivity for prediction emergency BAS in our newborns that might indicate the impact of hypoxemia and blood flow redistribution on fetal myocardium in fetuses with shunt restriction [28, 29]. Our finding of a reduced FO/TSL ratio as predictive cardiac parameter for urgent atrial septostomy at birth is in concordance with one recent study [8].

STRENGTH AND LIMITATIONS

Comprehensive cardiac evaluation with application of modern ultrasound modalities including novel assessment of fetal LV torsion was an advantage of this study. The strict methodology, the same manner of fetal and neonatal cardiac assessment and good reproducibility are additional strengths. The limitation of our study was a proportionately small number of TGA pregnancies (n=13). However, the study power was sufficient to demonstrate significant alterations in cardiac parameters in this study group. Our preliminary findings of predictive

values of novel and conventional cardiac indices in TGA term fetuses for urgent BAS in neonates prompt further investigations of this issue in larger prospective studies.

CONCLUSIONS

Our results demonstrated that TGA term fetuses and neonates exhibited altered cardiac phenotype and different functional perinatal adaptation with evidence of more globular hypertrophied ventricles, markedly increased biventricular systolic contractility and diastolic dysfunction prenatally with more profound alterations in these cardiac parameters after birth. These findings are suggestive of cardiac adaptation to the abnormal loading conditions of TGA as a consequence of blood flow redistribution at term and persistence of abnormal parallel arrangement of cardiovascular circulation postnatally. Several cardiac indices in TGA term fetus showed high sensitivity and specificity for prediction of urgent BAS after birth reflecting compensatory cardiovascular responses to late-gestation pathophysiology and fetal hypoxemia. If our findings of predictive values of fetal cardiac parameters for urgent BAS in TGA neonates are validated in larger prospective studies, the detailed cardiac assessment of TGA fetuses near term could facilitate improved perinatal management and pregnancy outcome.

ACKNOWLEDGEMENTS

We are grateful to Emeritus Professor of Paediatrics Abraham Morris Rudolph for his interest in our research, invaluable help in reviewing study findings, and his intellectual input to the manuscript context. We acknowledge all patients that have taken part in this study, General Electric Ultrasound Company for providing ultrasound platform and software for this research, and all medical staff of the Fetal Medicine Unit of St George's Hospital, and Paediatric Cardiology and Brompton Centre for Fetal Cardiology of the Royal Brompton Hospital for their contribution to patient's recruitment.

CONFLICT OF INTERETS

The authors report no conflict of interest.

FUNDING SOURCES

Dr Olga Patey was partly supported by Children's Heart Unit Fund (CHUF), Royal Brompton and Harefield Hospital Charity (registered no. 1053584), and by SPARKS Charity (registered no.1003825, grant ref. no.14EDI01).

REFERENCES

1. Samanek M. Congenital heart malformations: prevalence, severity, survival, and quality of life. *Cardiol Young* 2000; **10**: 179-185.

2. Villafane J, Lantin-Hermoso MR, Bhatt AB, Tweddell JS, Geva T, Nathan M, Elliott MJ, Vetter VL, Paridon SM, Kochilas L, Jenkins KJ, Beekman RH, 3rd, Wernovsky G, Towbin JA. D-transposition of the great arteries: the current era of the arterial switch operation. *J Am Coll Cardiol* 2014; **64**: 498-511.

3. Martins P, Castela E. Transposition of the great arteries. *Orphanet J Rare Dis* 2008; **3**: 27.

4. Maeno YV, Kamenir SA, Sinclair B, van der Velde ME, Smallhorn JF, Hornberger LK. Prenatal features of ductus arteriosus constriction and restrictive foramen ovale in d-transposition of the great arteries. *Circulation* 1999; **99**: 1209-1214.

5. Jouannic JM, Gavard L, Fermont L, Le Bidois J, Parat S, Vouhe PR, Dumez Y, Sidi D, Bonnet D. Sensitivity and specificity of prenatal features of physiological shunts to predict neonatal clinical status in transposition of the great arteries. *Circulation* 2004; **110**: 1743-1746.

6. Punn R, Silverman NH. Fetal predictors of urgent balloon atrial septostomy in neonates with complete transposition. *J Am Soc Echocardiogr* 2011; **24**: 425-430.

7. Porayette P, van Amerom JF, Yoo SJ, Jaeggi E, Macgowan CK, Seed M. MRI shows limited mixing between systemic and pulmonary circulations in foetal transposition of the great arteries: a potential cause of in utero pulmonary vascular disease. *Cardiol Young* 2015; **25**: 737-744.

8. Vigneswaran TV, Zidere V, Miller OI, Simpson JM, Sharland GK. Usefulness of the Prenatal Echocardiogram in Fetuses With Isolated Transposition of the Great Arteries to Predict the Need for Balloon Atrial Septostomy. *Am J Cardiol* 2017; **119**: 1463-1467.

9. Słodki M, Axt-Fliedner R, Zych-Krekora K, Wolter A, Kawecki A, Enzensberger C, Gulczyńska E, Respondek-Liberska M. New method to predict need for Rashkind procedure in fetuses with dextro-transposition of the great arteries. *Ultrasound Obstet Gynecol* 2018; **51**: 531-536.

10. Buca D, Winberg P, Rizzo G, Khalil A, Liberati M, Makatsariya AS, Greco F, Nappi L, Acharya G, D'Antonio F. Prenatal risk factors for urgent atrial septostomy at birth in fetuses with transposition of the great arteries: a systematic review and meta-analysis. *Journal of Maternal-Fetal and Neonatal Medicine* 2020.

11. Vaujois L, Boucoiran I, Preuss C, Brassard M, Houde C, Fouron JC, Raboisson MJ. Relationship between interatrial communication, ductus arteriosus, and pulmonary flow patterns in fetuses with transposition of the great arteries: prediction of neonatal desaturation. *Cardiol Young* 2017; **27**: 1280-1288.

12. Tuo G, Paladini D, Montobbio G, Volpe P, Cheli M, Calevo MG, Marasini M. Prenatal Echocardiographic Assessment of Foramen Ovale Appearance in Fetuses with D-Transposition of the Great Arteries and Impact on Neonatal Outcome. *Fetal Diagn Ther* 2017; **42**: 48-56.

13. Blanc J, Fouron JC, Sonesson SE, Raboisson MJ, Huggon I, Gendron R, Berger A, Brisebois S. Ventricular outputs, central blood flow distribution and flow pattern through the aortic isthmus of fetuses with simple transposition of the great arteries. *Acta Obstet Gynecol Scand* 2016; **95**: 629-634.

14. Godfrey ME, Friedman KG, Drogosz M, Rudolph AM, Tworetzky W. Cardiac output and blood flow redistribution in the fetus with D-loop transposition of the great arteries and intact ventricular septum: insights into the pathophysiology. *Ultrasound Obstet Gynecol* 2017; **50**: 612-617.

15. Lachaud M, Dionne A, Brassard M, Charron MA, Birca A, Dehaes M, Raboisson MJ. Cardiac hemodynamics in fetuses with transposition of the great arteries and intact ventricular septum from diagnosis to end of pregnancy: a longitudinal follow-up. *Ultrasound Obstet Gynecol* 2019.

16. Walter C, Soveral I, Bartrons J, Escobor MC, Carretero JM, Gomez O, Sanchez-de-Toledo J. Comprehensive Functional Echocardiographic Assessment of Transposition of the Great Arteries: From Fetus to Newborn. *Pediatr Cardiol* 2020 (in press).

17. Bonnet D, Coltri A, Butera G, Fermont L, Le Bidois J, Kachaner J, Sidi D. Detection of transposition of the great arteries in fetuses reduces neonatal morbidity and mortality. *Circulation* 1999; **99**: 916-918.

18. Rudolph AM. Aortopulmonary transposition in the fetus: speculation on pathophysiology and therapy. *Pediatr Res* 2007; **61**: 375-380.

19. Donofrio MT, Skurow-Todd K, Berger JT, McCarter R, Fulgium A, Krishnan A, Sable CA. Risk-Stratified Postnatal Care of Newborns with Congenital Heart Disease Determined by Fetal Echocardiography. *J Am Soc Echocardiogr* 2015; **28**: 1339-1349.

20. Crispi F, Bijnens B, Sepulveda-Swatson E, Cruz-Lemini M, Rojas-Benavente J, Gonzalez-Tendero A, Garcia-Posada R, Rodriguez-Lopez M, Demicheva E, Sitges M, Gratacos E. Postsystolic shortening by myocardial deformation imaging as a sign of cardiac adaptation to pressure overload in fetal growth restriction. *Circ Cardiovasc Imaging* 2014; **7**: 781-787.

21. Ingul CB, Loras L, Tegnander E, Eik-Nes SH, Brantberg A. Maternal obesity affects fetal myocardial function as early as in the first trimester. *Ultrasound Obstet Gynecol* 2016; **47**: 433-442.

22. Crepaz R, Secchieri S, Svaluto G, Milanesi O, Pitscheider W, Gentili L, Rubino M, Stellin G. Echocardiographic evaluation of systolic and diastolic left ventricular function following arterial switch operation in the neonatal period for transposition of the great arteries. Midterm results. *G Ital Cardiol* 1997; **27**: 224-230.

23. Adhyapak SM, Mahala BK, Pujar SV, Shetty PK, Sharma R. Impact of left ventricular function on early outcomes after arterial switch for D-transposition of great arteries with intact ventricular septum. *Indian Heart J* 2007; **59**: 137-141.

24. Xie M, Zhang W, Cheng TO, Wang X, Lu X, Hu X. Left ventricular torsion abnormalities in patients after the arterial switch operation for transposition of the great arteries with intact ventricular septum. *Int J Cardiol* 2013; **168**: 4631-4637.

25. van Doesburg NH, Bierman FZ, Williams RG. Left ventricular geometry in infants with d-transposition of the great arteries and intact interventricular septum. *Circulation* 1983; **68**: 733-739.

26. Rodriguez-Lopez M, Cruz-Lemini M, Valenzuela-Alcaraz B, Garcia-Otero L, Sitges M, Bijnens B, Gratacos E, Crispi F. Descriptive analysis of the different phenotypes of cardiac remodeling in fetal growth restriction. *Ultrasound Obstet Gynecol* 2017; **50** 207-221.

27. Wilson AD, Rao S, Aeschlimann S. Normal fetal foramen flap and transatrial Doppler velocity pattern. *J Am Soc Echocardiogr* 1990; **3**: 491-494.

28. van Dalen BM, Tzikas A, Soliman OI, Heuvelman HJ, Vletter WB, Ten Cate FJ, Geleijnse ML. Assessment of subendocardial contractile function in aortic stenosis: a study using speckle tracking echocardiography. *Echocardiography* 2013; **30**: 293-300.

29. Delhaas T, Kotte J, van der Toorn A, Snoep G, Prinzen FW, Arts T. I. Increase in left ventricular torsion-to-shortening ratio in children with valvular aortic stenosis. *Magn Reson Med* 2004: 135-139.

30. Patey O, Carvalho JS, Thilaganathan B. Left ventricular torsional mechanics in term fetuses and neonates. *Ultrasound Obstet Gynecol* 2020; **55** 233-241.

31. Patey O, Gatzoulis MA, Thilaganathan B, Carvalho JS. Perinatal Changes in Fetal Ventricular Geometry, Myocardial Performance, and Cardiac Function in Normal Term Pregnancies. *J Am Soc Echocardiogr* 2017; **30**: 485-492.e485.

32. Patey O, Carvaho JS, Thilaganathan B. Perinatal changes in cardiac geometry and function in growth restricted fetuses at term. *Ultrasound Obstet Gynecol* 2018; **53**: 655-662.

33. Patey O, Carvalho JS, Thilaganathan B. Perinatal changes in fetal cardiac geometry and function in gestational diabetic pregnancies at term. *Ultrasound Obstet Gynecol* 2019; **54**: 634-642.

34. Patey O. Re: Differential effect of assisted reproductive technology and small-for-gestational age on fetal cardiac remodeling. B. Valenzuela-Alcaraz, F. Crispi, M. Cruz-Lemini, B. Bijnens, L. Garcia-Otero, M. Sitges, J. Balasch and E. Gratacos. Ultrasound Obstet Gynecol. *Ultrasound Obstet Gynecol* 2017; **50**: 17-18.

35. Patey O, Carvalho JS, Thilaganathan B. Intervendor Discordance of Fetal and Neonatal Myocardial Tissue Doppler and Speckle-Tracking Measurements. *J Am Soc Echocardiogr* 2019; **32**: 1339-1349.

36. Rudolph AM. Congenital cardiovascular malformations and the fetal circulation. *Arch Dis Child Fetal Neonatal Ed* 2010; **95**: F132-136.

37. Konduri GG, Gervasio CT, Theodorou AA. Role of adenosine triphosphate and adenosine in oxygen-induced pulmonary vasodilation in fetal lambs. *Pediatr Res* 1993; **33**: 533-539.

38. Talemal L, Donofrio MT. Hemodynamic consequences of a restrictive ductus arteriosus and foramen ovale in fetal transposition of the great arteries. *J Neonatal Perinatal Med* 2016; **9**: 317-320.

39. Rudolph AM. The fetal circulation and its adjustments after birth in congenital heart disease. *UCLA Forum Med Sci* 1970; **10**: 105-118.

40. McMurphy DM, Heymann MA, Rudolph AM, Melmon KL. Developmental changes in constriction of the ductus arteriosus: responses to oxygen and vasoactive agents in the isolated ductus arteriosus of the fetal lamb. *Pediatr Res* 1972; **6**: 231-238.

41. Hawkins J, Van Hare GF, Schmidt KG, Rudolph AM. Effects of increasing afterload on left ventricular output in fetal lambs. *Circ Res* 1989; **65**: 127-134.

42. Gilbert RD. Control of fetal cardiac output during changes in blood volume. *Am J Physiol* 1980; **238**: H80-86.

43. Baschat AA, Gembruch U. Development of fetal cardiac and extracardiac Doppler flow in early gestation. Fetal Cardiology, Yagel S, Silverman NH, Gembruch U (Eds), Informa Healthcare *USA* 2009; 2nd ed: 152-171.

44. Brooks PA, Khoo NS, Mackie AS, Hornberger LK. Right ventricular function in fetal hypoplastic left heart syndrome. *J Am Soc Echocardiogr* 2012; **25**: 1068-1074.

45. Brooks PA, Khoo NS, Hornberger LK. Systolic and diastolic function of the fetal single left ventricle. *J Am Soc Echocardiogr* 2014; **27**: 972-977.

46. Jonker SS, Giraud MK, Giraud GD, Chattergoon NN, Louey S, Davis LE, Faber JJ, Thornburg KL. Cardiomyocyte enlargement, proliferation and maturation during chronic fetal anaemia in sheep. *Exp Physiol* 2010; **95**: 131-139.

47. Toischer K, Rokita AG, Unsold B, Zhu W, Kararigas G, Sossalla S, Reuter SP, Becker A, Teucher N, Seidler T, Grebe C, Preuss L, Gupta SN, Schmidt K, Lehnart SE, Kruger M,

Linke WA, Backs J, Regitz-Zagrosek V, Schafer K, Field LJ, Maier LS, Hasenfuss G. Differential cardiac remodeling in preload versus afterload. *Circulation* 2010; **122**: 993-1003.

48. Hauton D, Ousley V. Prenatal hypoxia induces increased cardiac contractility on a background of decreased capillary density. *BMC Cardiovasc Disord* 2009; **9**: 1.

49. Jonker SS, Giraud GD, Espinoza HM, Davis EN, Crossley DA. Effects of chronic hypoxia on cardiac function measured by pressure-volume catheter in fetal chickens. *Am J Physiol Regul Integr Comp Physiol* 2015; **308**: R680-689.

50. Fulton DR, Fyler DC. D-Transposition of the Great Arteries. . *Nadas' Pediatric Cardiology* 2006; Keane JF, Lock JE, Fyler DC (Eds), Saunders Elsevier, Philadelphia, PA. .

51. Lalezari S, Hazekamp MG, Bartelings MM, Schoof PH, Gittenberger-De Groot AC. Pulmonary artery remodeling in transposition of the great arteries: relevance for neoaortic root dilatation. *J Thorac Cardiovasc Surg* 2003; **126**: 1053-1060.

52. Johnson RC, Datar SA, Oishi PE, Bennett S, Maki J, Sun C, Johengen M, He Y, Raff GW, Redington AN, Fineman JR. Adaptive right ventricular performance in response to acutely increased afterload in a lamb model of congenital heart disease: evidence for enhanced Anrep effect. *Am J Physiol Heart Circ Physiol* 2014; **306**: H1222-1230.

53. Minegishi S, Kitahori K, Murakami A, Ono M. Mechanism of pressure-overload right ventricular hypertrophy in infant rabbits. *Int Heart J* 2011; **52**: 56-60.

54. Kameny RJ, He Y, Morris C, Sun C, Johengen M, Gong W, Raff GW, Datar SA, Oishi PE, Fineman JR. Right ventricular nitric oxide signaling in an ovine model of congenital heart disease: a preserved fetal phenotype. *Am J Physiol Heart Circ Physiol* 2015; **309**: H157-165.

55. Bogaard HJ, Abe K, Vonk Noordegraaf A, Voelkel NF. The right ventricle under pressure: cellular and molecular mechanisms of right-heart failure in pulmonary hypertension. *Chest* 2009; **135**: 794-804.

56. Jonker SS, Louey S. Endocrine and other physiologic modulators of perinatal cardiomyocyte endowment. *J Endocrinol* 2016; **228**: R1-18.

57. Molina CE, Johnson DM, Mehel H, Spatjens RL, Mika D, Algalarrondo V, Slimane ZH, Lechene P, Abi-Gerges N, van der Linde HJ, Leroy J, Volders PG, Fischmeister R, Vandecasteele G. Interventricular differences in beta-adrenergic responses in the canine heart: role of phosphodiesterases. *J Am Heart Assoc* 2014; **3**: e000858.

58. Mital S. Right ventricle in congenital heart disease: is it just a "weaker" left ventricle? *Arch Mal Coeur Vaiss* 2006; **99**: 1244-1251.

59. Lai CT, Chow PC, Wong SJ, Chan KW, Cheung YF. Circulating annexin A5 levels after atrial switch for transposition of the great arteries: relationship with ventricular deformation and geometry. *PLoS One* 2012; **7**: e52125.

60. Fisher DJ, Heymann MA, Rudolph AM. Fetal myocardial oxygen and carbohydrate consumption during acutely induced hypoxemia. *Am J Physiol* 1982; **242**: H657-661.

61. Chaoui R. Coronary arteries in fetal life: physiology, malformations and the "heart-sparing effect". *Acta Paediatr Suppl* 2004; **93**: 6-12.

62. Rudolph AM. Impaired cerebral development in fetuses with congenital cardiovascular malformations: Is it the result of inadequate glucose supply? *Pediatr Res* 2016; **80**: 172-177.

63. Laser KT, Haas NA, Fisher M, Habash S. Left ventricular rotation and right–left ventricular interaction in congenital heart disease: the acute effects of interventional closure of patent arterial ducts and atrial septal defects. *Cardiology in Young* 2014; **24**: 661-674.

Figure legends

Figure 1 Myocardial deformation indices in TGA term fetal and neonate compared to normal groups. (A) Speckle tracking myocardial deformational curve showing LV circumferential strain in TGA term fetus obtained from LV short axis view. The box-and-whiskers plots show alterations in (B) LV basal systolic circumferential strain [C-S] and (C) LV basal systolic circumferential strain rate [C-SR] in TGA groups compared to normal controls. Normal fetuses and neonates are shown *in white*, and TGA groups are *in black* colour. Boxes represent median and interquartile range, and whiskers are 5th and 95th centiles; *****, p-value < 0.001; †, p-value <0.01 compared normal term fetuses with TGA term fetuses, and normal neonate with TGA neonates; §, p-value <0.01 compared TGA fetuses with TGA neonates.

Figure 2 Summary of significant cardiac geometrical and functional alterations in TGA term fetuses and neonates compared to normal controls. The spiderweb plot showing significant alterations of cardiac parameters in TGA term fetuses *(in blue)* and TGA neonates *(in red)* compared to fetal and neonatal normal controls *(in green).* CO, cardiac output; CCO, combined cardiac output; C-SR, circumferential strain rate; IVRT', isovolumetric relaxation time; L-S, longitudinal strain; LV, left ventricular; RV, right ventricular; S', systolic myocardial velocities; SI, sphericity index.

Figure 3 Significantly different fetal cardiac parameters in non-BAS vs BAS TGA term fetuses. The box-and-whiskers plots show significant differences between non-BAS and BAS subgroups of TGA term fetuses in (A) LV rotation-to-shortening ratio [RSR], (B) RV/LV end-diastolic area ratio, (C) pulmonary valve to aortic valve dimension ratio, (D) RV/LV cardiac output ratio, and (E) foramen ovale shunt size to total interatrial septal length ratio [FO/TSL].

Non-BAS fetuses are shown *in white*, and BAS fetuses are *in black* colour. Boxes represent median and interquartile range, and whiskers are 5th and 95th centiles. *Rotation-to-shortening ratio (RSR) = LV apical systolic rotation / LV basal circumferential strain.*

Figure 4 Receiver Operating Characteristic (ROC) curves of fetal cardiac indices for prediction of emergency balloon atrial septostomy (BAS) in TGA neonates. ROC curves demonstrating sensitivity and specificity of cardiac parameters in TGA term fetuses for an urgent neonatal BAS prediction: LV rotation-to- shortening ratio [RSR] *(in red)*, pulmonary valve to aortic valve [PV/AV] dimension ratio *(in purple)*, RV to LV end-diastolic area ratio *(in turquoise),* foramen ovale to total interatrial septal length [FO/TSL] dimension ratio *(in yellow)*, RV/LV cardiac output [CO] ratio *(blue curve).*

Figure 5 Patterns of blood flow and percentages of the oxygen saturation in main vessels in (A) normal fetus and (B) fetus with simple TGA at term. The figure demonstrates considerably greater than normal oxygen saturation in the pulmonary artery in TGA term fetus, while oxygen saturation in the ascending aorta is less than normal (percentage of oxygen saturation is shown in blue circles). The oxygen saturations shown in normal term fetuses were derived from fetal lambs *in utero;* the assumptions of volumes of blood flow were used in calculating oxygen saturations in the main vessels in simple TGA term fetuses. Ao, aorta; LA, left atrium; LV, left ventricle; PA, pulmonary artery; RA, right atrium; RV, right ventricle. Adapted with permission from Rudolph [18].

Figure 6 Schematic representation of haemodynamic and ventricular loading conditions alterations in simple TGA fetuses at term. The diagram showing blood flow in

TGA term fetuses where alterations in oxygen delivery to pulmonary and cerebrovascular circulations in TGA malformation around time of birth can lead to blood flow redistribution and fetal shunt restriction resulting in both changes in cardiac loading conditions and, in proportion of fetuses, in systemic/pulmonary hypoxemia, thus impacting cardiac geometry and function. Ao, aorta; DA, ductus arteriosus; DV, ductus venosus; FO, foramen ovale; LA, left atrium; LV, left ventricle; PA, pulmonary artery; RA, right atrium; RV, right ventricle; UV, umbilical vein.

Supplemental figure legends

Figure S1 Cardiac indices in TGA term fetuses and neonates compared to normal groups and perinatal changes in TGA group.

Figure S2 Additional significantly different fetal cardiac parameters in non-BAS vs BAS TGA term fetuses.

Figure S3 Significant association between TGA fetal cardiac parameters predictive for urgent BAS after birth.

Supplemental tables

Table S1 Demographic characteristic of non-BAS vs BAS TGA term fetuses

Table S2 Perinatal changes in cardiac geometry and function in TGA term fetuses and neonates compared to normal groups with crude and normalized values.

Table S3. Intra- and inter-observer errors of fetal and neonatal cardia indices.

Table S4 Fetal studies assessing foramen ovale and ductus arteriosus in simple TGA.

TABLES

Table 1. Demographic characteristic of the study population

Parameters	Normal (n=54)	TGA (n=13)	p-value
Maternal characteristics			
Maternal age (years)	33 ± 5	29 ± 6	0.018
Ethnicity (number): Caucasian	35 (65%)	11 (85%)	0.151
Asian	15 (28%)	2 (15%)	
Afro-Caribbean	4 (7%)	0 (0%)	
Delivery mode (C-section) (number)	14 (26%)	8 (62%)	0.025
Gestational age at delivery (weeks)	40 ± 0.1	39 ± 0.6	0.092
Fetal cardiac assessment			
Gestational age (weeks)	38 (3)	38 (1)	0.129
Time gap between the fetal scan and birth (days)	10 (4)	8 (7)	0.097
Restrictive FO (number)	0 (0%)	7 (54%)	0.010
Neonatal cardiac assessment after birth (before ASO)			
Neonate's age at the time of scan (hours)	18 (13)	27 (21)	0.056
Neonate's sex (male) (number)	28 (52%)	11 (85%)	0.060
Neonate's weight (kilograms)	3.49 ± 0.44	3.29 ± 0.29	0.190
FO presence (number)	54 (100%)	13 (100%)	0.890
DA presence (number)	43 (79%)	13 (100%)	0.007
Tricuspid regurgitation presence (number)	3 (6%)	8 (62%)	0.008
Restrictive FO required BAS (number)	0 (0%)	7 (54%)	0.010
Restrictive DA (number)	0 (0%)	2 (15%)	0.116

Values are mean ± SD, median (interquartile range), or n (%); BAS, balloon atrial septostomy; DA, ductus arteriosus; FO, foramen ovale; TGA, transposition of the great arteries.

Table 2. Perinatal changes in cardiac geometry in TGA term fetuses and neonates compared to normal controls

Parameters	Fetus at term		Neonate	
	Normal	TGA	Normal	TGA
LV sphericity index	0.49 (0.06)	0.55 (0.07)†	0.50 (0.04)	0.54 (0.03)
RV sphericity index	0.54 (0.12)	0.58 (0.21)†	0.43 (0.03)	0.61 (0.04)*****
LAVV dimension, mm	8.84 ± 1.07	8.39 ± 1.39	9.82 ± 0.86	8.59 ±1.52*****
RAVV dimension, mm	10.46 ± 1.22	10.44 ± 0.71	9.26 ± 1.01	10.38 ± 1.31*****
RAVV/LAVV ratio	1.18 (0.21)	1.18 (0.49)	0.97 (0.08)	1.24 (0.20)*****
LV EDD, mm	14.08 ± 2.14	13.90 ± 2.20	16.83 ± 1.65	14.96 ± 2.61*****
RV EDD, mm	16.80 (2.70)	17.60 (2.30)	13.89 ± 1.54	17.33 ± 1.49*****
RV/LV EDD ratio	1.20 (0.21)	1.26 (0.28)	0.86 (0.12)	1.16 (0.21)*****
LV EDL, mm	29.44 ± 4.86	25.61 ± 4.64†	34.25 (5.1)	28.1 (4.0)*****
RV EDL, mm	30.54 ± 4.94	26.92 ± 3.87†	32.30 ± 3.23	29.81 ± 1.90†
IVS relative thickness	0.50 ± 0.13	0.78 ± 0.23*****	0.49 ± 0.14	0.78 ± 0.23*****
LV RWT	0.55 ± 0.24	0.60 ± 0.25*****	0.54 ± 0.13	0.76 ± 0.23*****
RV RWT	0.62 ± 0.12	0.97 ± 0.32*****	0.60 ± 0.16	0.85 ± 0.21*****
AV dimension, mm	7.67 ± 0.73	8.90 ± 1.20*****	8.20 ± 0.81	9.49 ± 1.21*****
PV dimension, mm	8.43 ± 0.76	8.16 ± 1.20	9.11 ± 0.68	8.48 ± 1.37†
PV/AV dimension ratio	1.08 (0.04)	1.00 (0.14)*****	1.10 (0.12)	0.88 (0.10)*****

Values are mean ± SD, median (interquartile range). EDL, end-diastolic length; LAVV, left atrioventricular valve; LV, left ventricular; RAVV, right atrioventricular valve; RV, right ventricular; RWT, relative wall thickness; TGA, transposition of the great arteries. *Relative wall*

thickness = (2 x wall thickness)/EDD. *****, p-value < 0.001; †, p-value <0.01 compared normal term fetuses with TGA term fetuses, and normal neonates with TGA neonates.

Table 3. Perinatal changes in cardiac function in TGA term fetuses and neonates compared to normal controls.

Parameters	Fetus at term		Neonate	
	Normal	TGA	Normal	TGA
Global myocardial performance				
LV MPI'	0.52 (0.14)	0.45 (0.16)	0.39 (0.11)	0.47 (0.13)†
RV MPI'	0.52 (0.13)	0.52 (0.19)	0.34 (0.06)	0.47 (0.09)*****
LV torsion, deg/cm	3.00 (3.10)	4.27 (3.96)†	1.40 (2.52)	1.10 (3.53)‡
Systolic function				
Heart rate, bpm	138 ± 9	141 ± 11	116 ± 13	146 ± 11*****
LV CO, ml/min/kg	197 (75)	220 (141)	269 (86)	299 (200)***§**
RV CO, ml/min/kg	213 (73)	273 (172)†	208 (68)	358 (167)***‡**
CCO, ml/min/kg	406 (100)	483 (162)†	486 (179)	697 (380)***‡**
LV S', cm/s	0.16 (0.12)	0.18 (0.06)	0.14 (0.07)	0.23 (0.09)***§**
IVS S', cm/s	0.13 (0.17)	0.15 (0.09)	0.13 (0.05)	0.19 (0.07)†**§**
RV S', cm/s	0.17 (0.11)	0.24 (0.09)†	0.20 (0.08)	0.31 (0.10)***‡**
LV ejection time', ms	371 (40)	425 (40)†	394 ± 40	436 ± 30*****
LV IVCT', ms	97 (11)	92 (20)	78 ± 14	93 ± 1*****
RV ejection time', ms	390 (84)	419 (5)†	434 (70)	447 (49)**§**
RV IVCT', ms	96 (52)	103 (38)	70 (15)	94 (3)*****
Diastolic function				
LV E'/A'	0.78 (0.24)	0.57 (0.27)	1.24 (0.27)	0.62 (0.21)*****
IVS E'/A'	0.71 (0.14)	0.78 (0.25)	1.03 ± 0.29	0.76 ± 0.15†

LV relaxation time', ms	410 ± 47	373 ± 53†	450 ± 63	378 ± 60*****
LV IVRT', ms	98 (30)	104 (24)	79 ± 16	100 ± 25*****
RV relaxation time', ms	398 (51)	372 (59)†	416 (81)	341 (85)*****
RV IVRT', ms	102 (33)	127 (30)†	71 (16)	106 (40)*****

Values are mean ± SD, median (interquartile range). A', atrial contraction myocardial diastolic peak velocity, derived by PW TDI; CO, cardiac output; CCO, combined cardiac output; E', early diastolic myocardial peak velocity derived by PW-TDI; EDD, end-diastolic dimension; IVCT', isovolumetric contraction time obtained by PW-TDI; IVS, interventricular septal; IVRT', isovolumetric relaxation time obtained by PW-TDI; LV, left ventricular; RV, right ventricular; TGA, transposition of the great arteries. Values are normalized by cardiac cycle length, ventricular end-diastolic length or EDD as appropriate. *****, p-value < 0.001; †, p-value <0.01 compared normal term fetuses with TGA term fetuses, and normal neonates with TGA neonates; ‡, p-values < 0.001 and §, p-value <0.01 compared TGA fetuses with TGA neonates.

Table 4. Summary of significant alterations in cardiac parameters in TGA term fetuses and neonates compared to normal groups and significant perinatal changes in TGA group

Cardiac geometry	Myocardial deformation	Systolic function	Diastolic function
TGA term fetuses compared to Normal term fetuses			
↑LV and RV sphericity	↑RV longitudinal strain	↑RV systolic velocities S'	↓LV and RV relaxation time'
↑IVS, LV and RV relative wall thickness	↑LV_{basal} circumferential strain and systolic strain rate	↑LV and RV ejection time'	↑RV IVRT'
↑Aortic valve dimension	↑LV_{basal} radial strain and systolic strain rate	↑RV CO and CCO	
	↑LV torsion		
TGA neonates compared to Normal neonates			
↑RV sphericity	↑LV and RV longitudinal strain and systolic strain rate	↑Heart rate	↓LV and RV E/A (<1)
↓LV end-diastolic dimension	↑$LV_{basal\ \&\ apical}$ circumferential strain and systolic strain rate	↑LV and RV CO, and CCO	↓LV and IVS E'/A' (<1)
↓LV end-diastolic length	↑LV_{basal} radial strain and systolic strain rate	↑LV, RV and IVS systolic velocities S'	↓LV and RV relaxation time'
↑IVS, LV and RV relative wall thickness	↑LV and RV MPI'	↑LV ejection time'	↑LV and RV IVRT'
↑Aortic valve and ↓Pulmonary valve dimensions	↑MAPSE and SAPSE	↑LV and RV IVCT'	
Perinatal changes in TGA group (TGA term fetuses compared to TGA neonates)			
	↑LV_{basal} circumferential strain	↑LV and RV CO, and CCO	
	↑LV_{basal} radial strain	↑LV, RV and IVS S'	
	↓LV torsion	↑RV ejection time'	

CCO, combined cardiac output; CO, cardiac output; E/A, transvalvular early diastolic velocity to late atrial contraction velocity ratio obtained by PW Doppler; E'/A', early diastolic myocardial velocity to late atrial contraction myocardial velocity ratio; IVCT', isovolumetric contraction time by PW-TDI; IVRT', isovolumetric relaxation time; IVS, interventricular septum; LV, left

ventricle; MAPSE, mitral annular plane systolic excursion; MPI', myocardial performance index; RV, right ventricle; S', myocardial systolic velocities; SAPSE, septal annular plane systolic excursion; TGA, transposition of the great arteries; all indices with (') are obtained by PW-TDI.

Table 5. Predictive values of fetal cardiac indices for restrictive foramen ovale required emergency balloon atrial septostomy in TGA neonates

Parameters	LV apical rotation-to-shortening ratio *(LV RSR)*	RV/LV end-diastolic area ratio *(RV/LV EDA)*	Pulmonary valve to aortic valve dimension ratio *(PV/AV)*	RV/LV cardiac output ratio *(RV/LV CO)*	FO size to total interatrial septal length ratio *(FO/TSL)*
Area under curve (AUC)	0.94	0.98	0.98	0.95	0.93
AUC 95% CI	0.81 - 1.00	0.90 - 1.00	0.90 - 1.00	0.84 - 1.00	0.78 - 1.00
P-value	0.009	0.004	0.004	0.007	0.010
Cut-off value	≥ 0.23	≥ 1.33	≤ 0.89	≥ 1.38	≤ 0.27
Sensitivity (95% CI), %	100 (52 - 100)	86 (42 - 99)	86 (42 - 99)	86 (42 - 99)	86 (42 - 99)
Specificity (95% CI), %	83 (37 - 99)	100 (52 - 100)	100 (52 - 100)	83 (37 - 99)	83 (37 - 99)
Likelihood Ratio	11	12	12	9	9

CI, confidence interval; LV, left ventricular; RV, right ventricular. *Rotation-to-shortening ratio (RSR) = LV apical rotation / LV basal circumferential strain.*

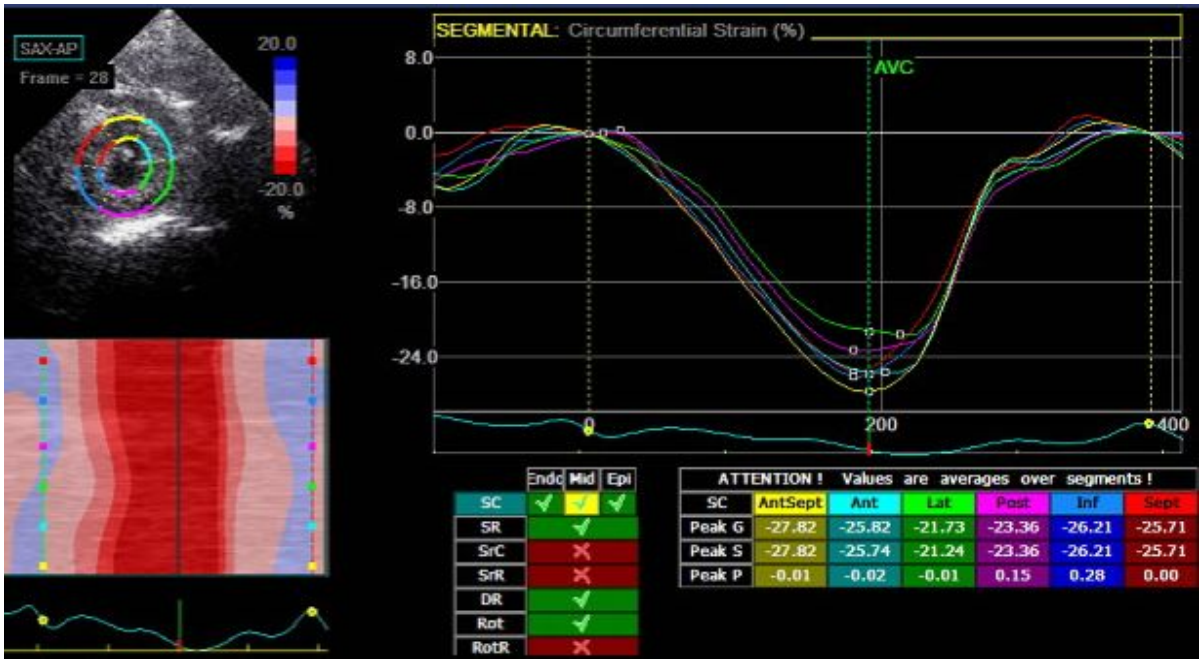

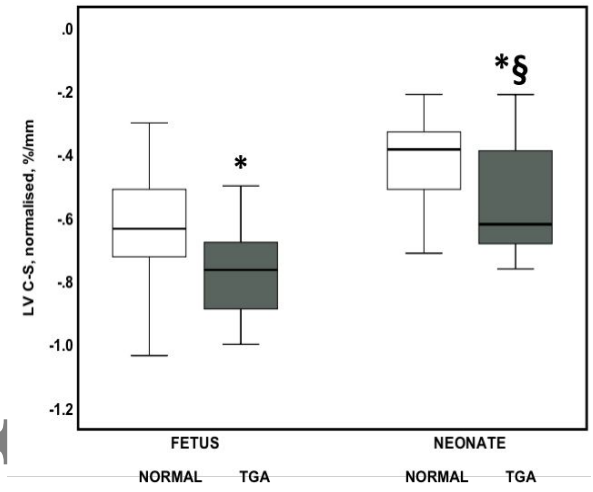

A.

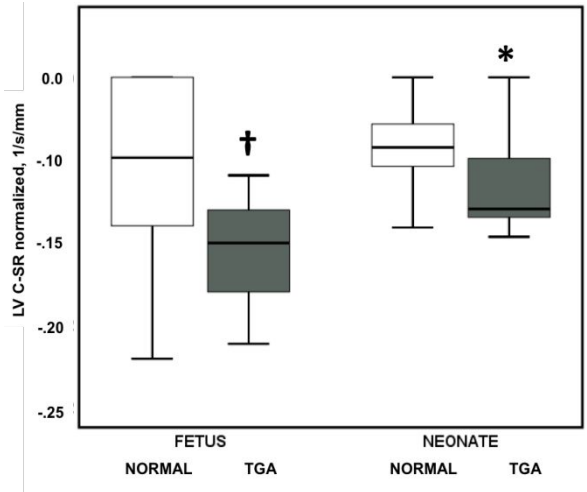

B.

Figure 1.

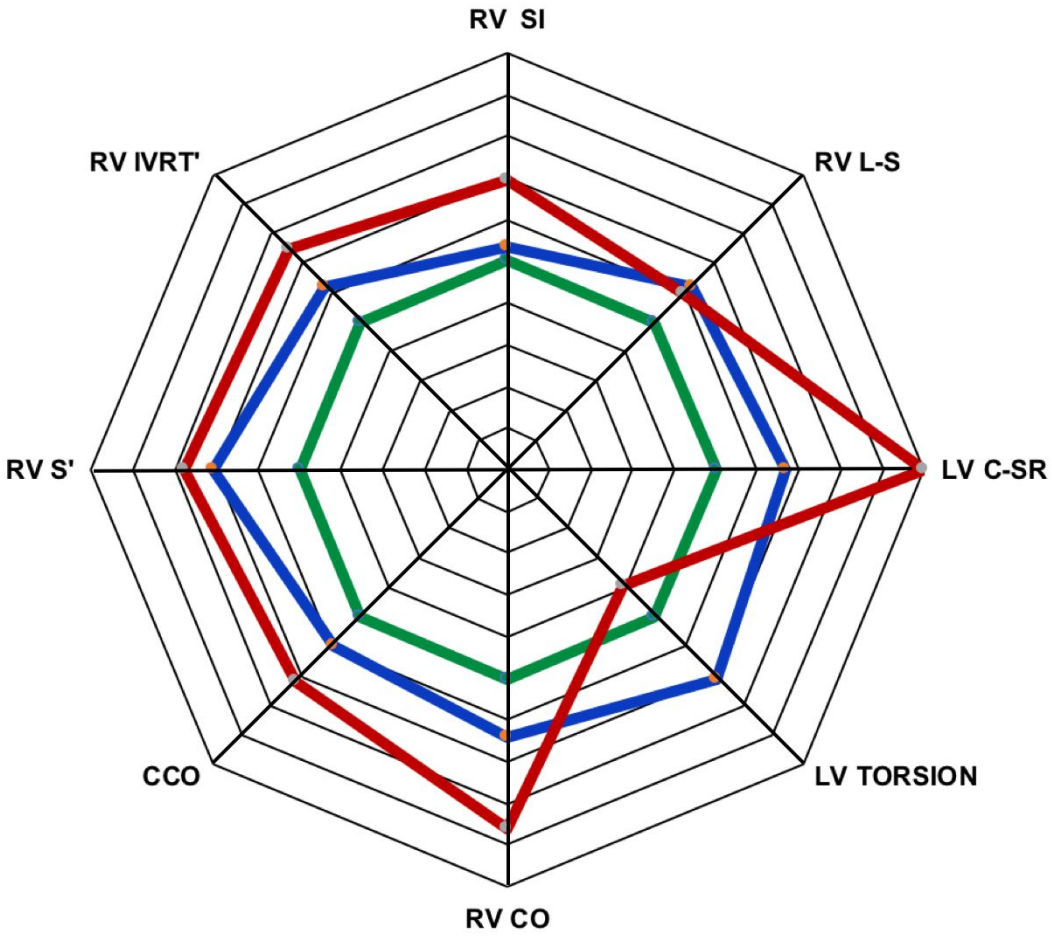

Figure 2.

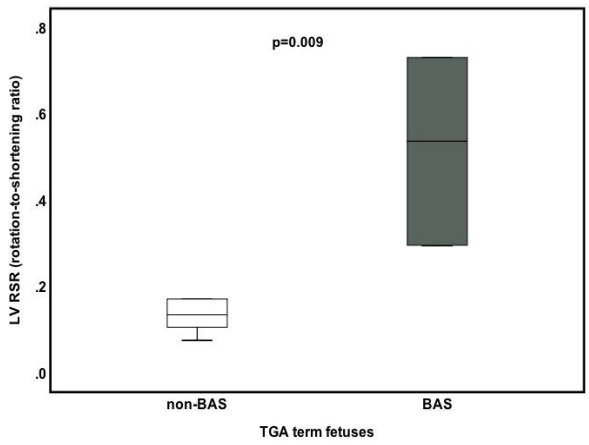

A.

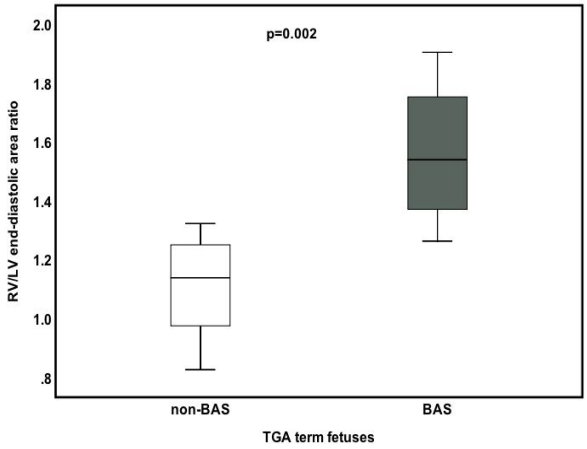

B.

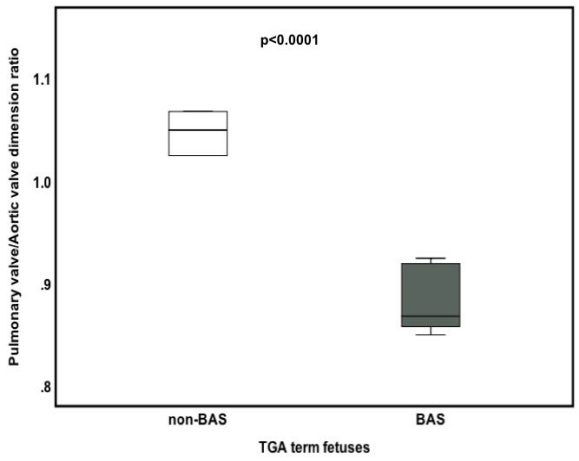

C.

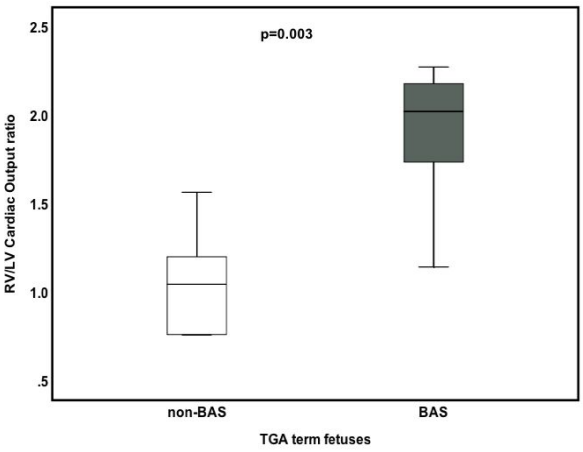

D.

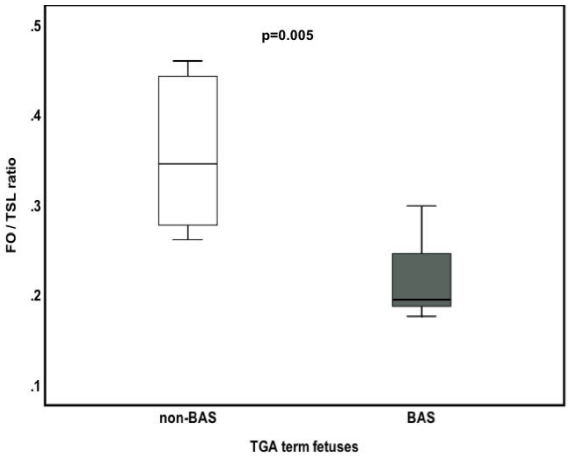

E.

Figure 3.

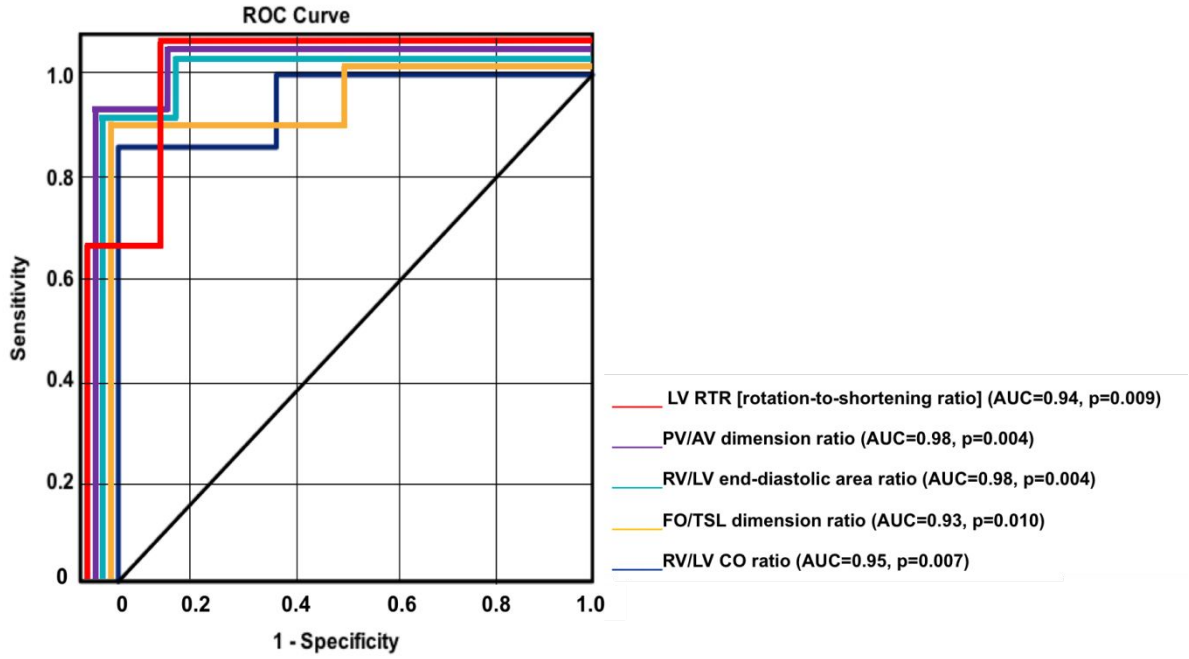

Figure 4.

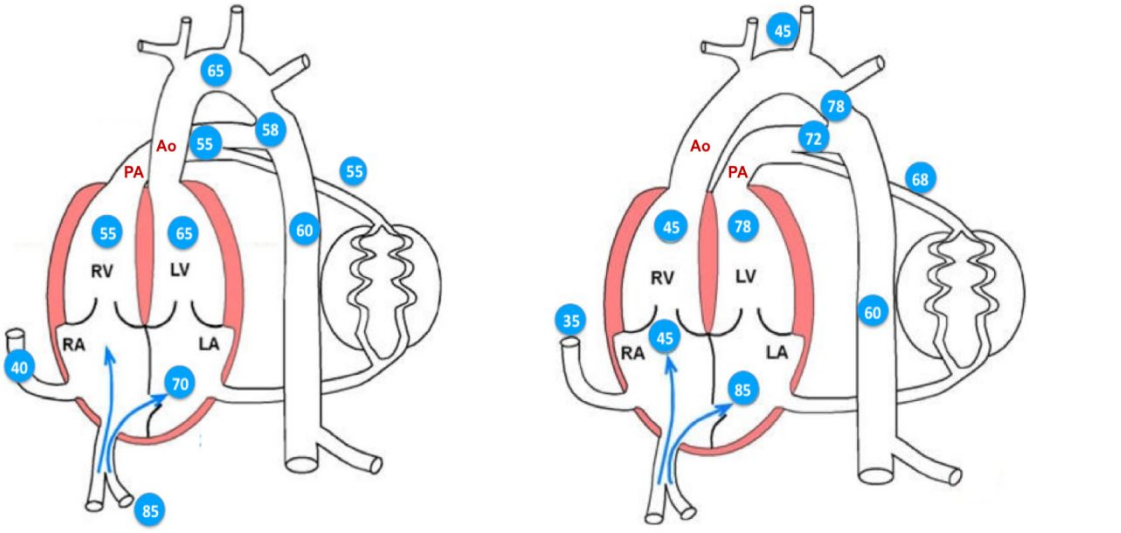

Normal term fetus

Simple TGA term fetus

A. **B.**

Figure 5.